

HEAT EXCHANGER MODELING METHODS FOR HYDROGEN POWERED AERO ENGINES DURING THERMODYNAMIC CYCLE DESIGN

Alexander Görtz, Jannik Häßy, Marc Baier Schmelcher, Mahmoud El-Soueidan & Florian Herbst

German Aerospace Center (DLR), Linder Höhe, 51147 Cologne, Germany

Abstract

Aviation is responsible for a growing portion of global greenhouse gas emissions contributing to climate change and hydrogen is a promising fuel alternative for reducing the climate impact of aviation. Hydrogen requires a complex pre-conditioning system utilizing multiple heat exchangers in a secondary fluid cycles. Many options for heat exchanger modeling methods are available which have impact on system- and component-level results. This paper investigates three different modeling methods (correlations, map and coupling a tool of higher order). All methods are applied to the exhaust gas heat exchanger of the LH2 pre-conditiong system during thermodynamic cycle calculation. The results are compared on both levels and a recommendation for a specific method is given. While all methods provide good results on system level, it is recommended to use correlations for the analysis of large parameter variations and to use the coupling method for preliminary design where specific geometries and weights are required.

Keywords: Propulsion, Aero Engine, Engine Performance, Hydrogen, Heat Exchanger

1. Introduction

The reduction of greenhouse gas emissions is one of the most important challenges for the aviation industry today [1]. Conventional kerosene-fueled aircraft engines contribute significantly to global CO2 emissions, motivating the search for alternative energy carriers that enable more sustainable flight. Among the possible solutions, hydrogen is a particularly promising candidate due to its potential to eliminate CO2 emissions during flight. Hydrogen as fuel has been of interest in the early 90s as Brewer [2] provided insights to hydrogen powered aircraft and also in the 2000s with the "Cryoplane" project [3]. More recent literature focus on the integration of hydrogen systems into the core engine and on the overall demonstration of hydrogen powered gas turbine engines [4, 5]. However, the adoption of hydrogen as an aviation fuel is not a straightforward substitution. Especially liquid hydrogen (LH2) requires cryogenic storage at around 20 K, which fundamentally changes the design requirements of both the aircraft and its propulsion system. While new aircraft configurations need to include the LH2 tanks, an additional challenge lies in the required overhaul of the engine architecture. A major driver of this overhaul is the hydrogen pre-conditioning system, which must safely and efficiently manage the thermal state of the fuel before combustion while interacting with multiple subsystems of the engine. Hydrogen itself offers the potential to reduce thrust specific energy consumption and making it an attractive option from a thermodynamic perspective. The different exhaust gas properties allow for increased working capability in the turbine section providing more power for propulsion. Nevertheless, integrating the hydrogen conditioning system into an aero engine introduces several challenges, particularly related to thermal management. Three possible installation positions of the heat source for the conditioning system have been evaluated in the past [6]. Those positions are inter compressor cooling (ICC), cooled cooling air (CCA) and exhaust cooling (EC).

While ICC provides the most benefits on a thermodynamic level, EC is more viable due to higher available temperature of the heat source and more installation space available. One critical issue arises from the extremely low temperatures from the liquid hydrogen, which pose a high risk of icing at the heat exchanger's walls. Such icing must be avoided at all costs, as it can severely degrade performance or even compromise engine safety. To mitigate this risk, the use of an intermediate or secondary fluid is proposed. However, introducing a secondary cycle significantly increases system complexity. It adds numerous new components to the engine, including multiple heat exchangers, liquid hydrogen pumps, compressors for the secondary fluid, and additional piping. Among these components, the heat exchanger used for EC is particularly challenging, as it is directly integrated into the core flow path of the engine.

From a modeling perspective, a wide range of heat exchanger modeling approaches exists in the literature. Simple NTU methods, scalable map-based models and high-fidelity cell-based or CFD approaches are all viable modeling options.

Modeling and integrating heat exchangers into gas turbine engines is not a new concept. Recuperative engine architectures have been investigated multiple times, for example by Boggia and Rüd [7] and also by Gonser [8] in the early 2000s. These studies primarily focused on air-to-air recuperators, where specific geometries were designed, analyzed and experimentally tested. More recent innovative concepts include the Water-Enhanced Turbofan, in which large heat exchangers and evaporators are integrated into the engine [9]. However, in these studies the off-design behavior was not investigated in detail, or as in the work of Ziegler et al., it was treated only in a highly simplified linearized manner [10]. Walsh and Fletcher [11] proposed a mass-flow-dependent modeling approach for heat exchangers, originally developed for air-to-air applications. This approach is also used in recent literature on hydrogen powered engines, although typically only one side of the heat exchanger is modeled in detail [12]. Other studies rely on strongly geometry-dependent methods, where a detailed heat exchanger geometry must be defined in advance [13]. To enable rapid performance estimation across a wide range of heat exchanger configurations, Milten et al. proposed a method based on existing data sets [14]. However, this approach still requires a sufficiently detailed specification of the heat exchanger geometry. Alternative analyses frequently employ CFD methods, which are both computationally expensive and dependent on an exact geometric definition, as demonstrated by Salpingidou [15]. While CFD methods provide detailed physical insight, they require a defined geometry and require substantial computational effort, making them unsuitable for engine cycle analysis and preliminary design phases.

In general, a common challenge arises from the fact that modeling approaches are either overly generic and simplified, or excessively detailed, requiring precise geometric information. When investigating a new propulsion concept, such as hydrogen propulsion with a LH2 pre-conditioning system, it is often unclear which heat exchanger modeling approach is most appropriate, particularly since the geometry should not yet be fixed at this stage of the design process. It is therefore essential to maintain the flexibility to specify the required heat flux at the design point without prescribing a specific geometry, while still being able to capture off-design behavior in a physically meaningful way. As a result, only three modeling approaches remain feasible for this application: NTU correlation methods, scalable maps, and cell-based approaches. This work investigates those three modeling methods for the exhaust gas heat exchanger in a hydrogen powered aero engine during thermodynamic cycle analysis. This paper will answer the following research questions:

- **RQ1:** What is the impact of the selected heat exchanger modeling method on engine level results, e.g. on thrust specific fuel consumption, overall transferred heat, and component operating behavior?
- **RQ2**: What are the advantages and disadvantages of the respective method and are there any limits?
- **RQ3:** Which method is most suitable for heat exchanger modeling during the cycle analysis and preliminary design of an aero engine?

To address these questions, thermodynamic cycle calculations are performed with each modeling method using the performance program DLRp2 [16] within the simulation framework GTlab [17, 18].

2. Engine Architecture

The investigated engine architecture is an engine designed for a short-medium range (SMR) aircraft configuration. The propulsion system under consideration is a two-shaft turbofan with a booster compressor. Both turbines are cooled, and the nozzles are unmixed. The engine architecture, including the associated conditioning system, is illustrated in Figure 1. Such a complex architecture is necessary to prevent ice formation and to reduce the risk in the event of leakage.

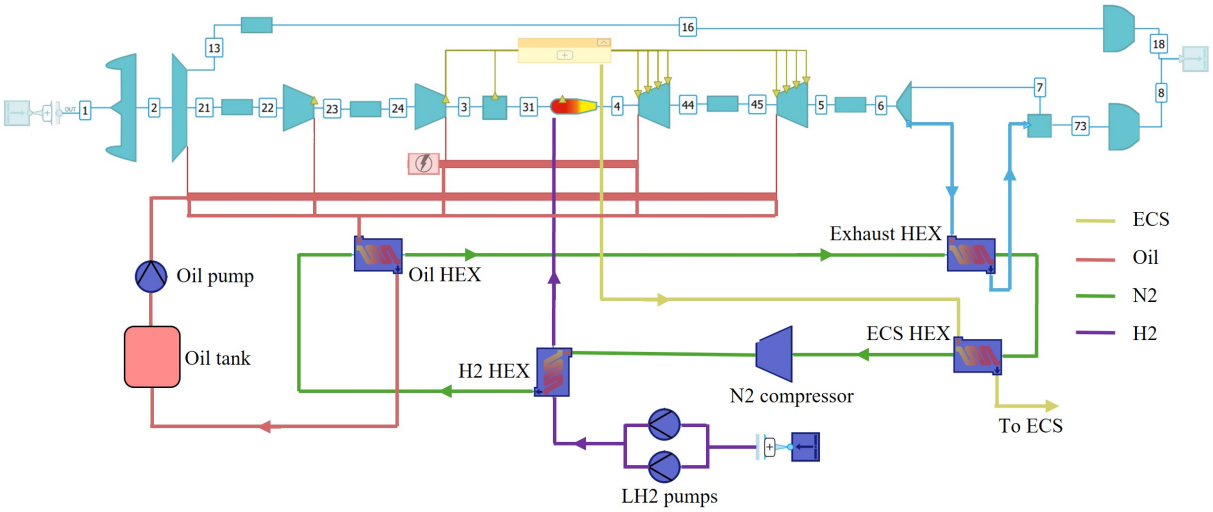


Figure 1 – Engine architecture with LH2 conditioning system concept [19]

The engine boundary is defined by an aircraft–engine interface, where liquid hydrogen is supplied from the aircraft distribution system to the engine. For simplification, a constant thermodynamic state of the LH2 at this interface is assumed during the entire flight mission. Liquid hydrogen is considered to be always available in sufficient quantity, at a pressure of 5 bar and a temperature of 25 K. This assumption allows the hydrogen tank and the low-pressure pump to be neglected. Entering the scope of the engine, the hydrogen pressure is increased to the injection pressure by high-pressure pumps (LH2 pumps). Pressures above 13 bar are required, at which point the hydrogen enters a supercritical state, making the distinction between liquid and gaseous phases irrelevant. At least two pumps are necessary to achieve this pressure increase. However, three pumps will be installed for redundancy. This is due to the large variations in hydrogen mass flow between operating points (see Sections 3.2 and 3.1). Current pumps reported in the literature are unable to deliver sufficient mass flow at the required pressure, necessitating the parallel operation of two pumps. After compression, the hydrogen is heated to reach the temperature required for combustion. Maximizing the heat transferred to the hydrogen is crucial for achieving a more efficient engine cycle. This heating is carried out in a designated heat exchanger (H2 HEX). Once fully conditioned in terms of pressure and temperature, the hydrogen is fed to the combustion chamber. To enable the heat transfer from the engines core to the hydrogen, a secondary fluid is required. Nitrogen is used as the working fluid in the secondary cycle. The H2 HEX heat exchanger uses the heat of the hot nitrogen to preheat the hydrogen. After transferring heat to the fuel, the nitrogen flows through multiple heat sources, accumulating heat in the engine to ultimately transfer it to the hydrogen in the H2 HEX. These heat sources include (i) engine oil (Oil HEX), (ii) a percentage of the turbine exhaust downstream of the low-pressure turbine (Exhaust HEX), and (iii) air for the Environmental Control System (ECS HEX). To ensure a sufficient mass flow rate in the secondary cycle, a compressor is required. While its primary function is to circulate the nitrogen, it also raises its temperature, enhancing the heat transfer to the hydrogen. This architecture of the pre-conditioning systems reduces the risk of icing because the temperature differences in the Exhaust HEX are low enough to prevent temperatures below 0 °C at the walls of this specific heat exchanger. In addition, hydrogen will never cross the exhaust gas or the core engine. In case of a leakage, no hydrogen will flow into the hot section of the engine.

3. Methodology

In this section modeling methods are explained for the specific engine design of a hydrogen powered aero engine during thermodynamic cycle design. The focus is on the hydrogen pre-conditioning system modeling methods as these differ from standard approaches for the cycle analysis of kerosene powered aero engines.

3.1 Engine Performance

The presented engine is designed for thrust requirements specific for a hydrogen SMR aircraft configuration. The thrust requirements are listed in Table 1. For this work three operating points are used during the cycle design. Cruise as the main design point where the engine is supposed to be as efficient as possible, Maximum Take-Off (MTO) where the highest temperatures occur and Top of Climb (TOC) with the highest reduced velocities in the engine's turbomachinery.

Table 1 – Thrust requirements [19]

Value	Unit	**Cruise**	**MTO**	**TOC**
Thrust	kN	23.7	139.6	26.3
Altitude	m	11277	0	10668
Mach Number	-	0.78	0	0.76
Temperature above ISA	K	0	15	10
Cabin Bleed Air	kg/s	0.425	0	0.425
Power Off-Take	kW	50	95	50

For all operating points, rules are applied to achieve specific design values or operational constrains. The pre-conditioning system is sized for cruise while taking off-design operating into account. The following rules are applied:

Heat Flux: The fuel temperature is the main design value for the size of the pre-conditioning system. This temperature determines how much heat has to be transferred in total to the hydrogen. A temperature of 300 K is set and the heat flux of the H2 HEX ($\dot{Q}_{\text{H2 HEX}}$) is a direct result of this specification. The sum of all heat sources is equal to the transferred heat to the hydrogen to reach a temperature of 300 K, see Equation 1

$$\dot{Q}_{\text{H2 HEX}} = \dot{Q}_{\text{Oil HEX}} + \dot{Q}_{\text{Exhaust HEX}} + \dot{Q}_{\text{ECS HEX}} + \dot{P}_{\text{W, N2Compressor}}. \tag{1}$$

The available heat of the oil system $\dot{Q}_{\text{Oil HEX}}$ is equal to the heat that is required to cool the engines oil. The heat for the ECS $\dot{Q}_{\text{ECS HEX}}$ is calculated by cooling the cabin bleed air. Hot air is extracted from the high-pressure compressor for the cabin. Which is then cooled to approx. 450 K. The power of the compressor $\dot{P}_{\text{W, N2Compressor}}$ is dependent on the pressure losses of the heat exchangers as this pressure drop has to be overcome to ensure nitrogen flow. During off design operating, the overall heat and fuel temperature is a result of pre-conditioning system. The remaining heat flux comes from the exhaust $\dot{Q}_{\text{Exhaust HEX}}$.

LH2 Pressure: The pressure ratio of the LH2 pump is defined by the hydrogen pressure at the injection point in the combustion chamber. For this analysis, a pressure of 60 bar of the hydrogen is set for cruise. The pressure ratio of fuel pressure and the pressure of the air at combustor inlet $dp_{\text{injection}} = \frac{p_{\text{fuel}}}{p_3}$ is set constant for all operating points at high altitude. For highly loaded operating point at sea level, the pressure ratio is set to $dp_{\text{injection}} = 2$ to ensure safe combustion. This means that there is still sufficient overpressure compared to the combustion chamber and the operating point of the LH2 pump has a similar surge margin in the component map. Due to the component map of the LH2 pump, see Figure 2, one pump is being used for flight at high altitudes and two pumps being required for high power sea level conditions.

Secondary Cycle: While the nitrogen mass flow is identical for all components in the secondary cycle, the pressure and temperature is different at each position. The pressure and temperature has to be set at exactly one position, the remaining positions are results from heat fluxes and pressure losses. Optimizing the engine architecture is not scope of this paper, therefore reasonable values for nitrogen mass flow, pressure and temperature are chosen based on the following guidelines. It can be beneficial for a heat exchanger to have a linear temperature profile to reduces locally high temperature differences. Therefore, the nitrogen mass flow is set to achieve the same enthalpy flow on both sides at the Exhaust HEX $R = \frac{\dot{m}_{\mathrm{N2}} \cdot c_{p,\mathrm{N2}}}{\dot{m}_{\mathrm{Exhaust}} \cdot c_{p,\mathrm{Exhaust}}} = 1$. The exhaust flow is separated downstream of the low-pressure turbine so 10 % of the core flow is passing through the heat exchanger. To reduce the mechanical stresses at the H2 HEX, the pressure of the hydrogen and nitrogen side is set to be equal at the design point. A nitrogen pressure of 60 bar is set at the entry in the H2 HEX. The N2 compressors pressure ratio is calculated accordingly to overcome the pressure losses in the secondary cycle. Reducing the risk of icing is the main reason for the secondary cycle. This can be achieved by ensuring the wall temperature of the Exhaust HEX cannot be below 273 K. Therefore, the N2 temperature at the HEX entry is set to 273 K guaranteeing that the wet exhaust flow will not freeze. For all off-design points additional rules are applied. Component maps for all compressors and the LH2 pumps are used to describe their operating behaviour. The N2 compressor is operated at a relative speed of 1.18. This rotational speed determines the compressor's delivery rate and thus the nitrogen mass flow. The heat fluxes of the heat exchangers are calculated using the respective method from Section 3.3 and the temperature of the nitrogen adjusts accordingly. However, an assumption must be made for the pressure in the secondary cycle. The goal is to avoid using a nitrogen tank. Therefore, the absolute amount of nitrogen is already defined in the design calculation. Within the scope of this work, it is not possible to calculate this amount, as this would require the exact geometry of all heat exchangers, pipes, etc. For simplicity, an average temperature $\overline{T}$ and average pressure $\overline{p}$ are determined in the secondary cycle. This is the average value from all stations in the nitrogen cycle, see Figure 1. The ideal gas equation is evaluated using these average values

$$\frac{\overline{p}_{\mathrm{CR}} \cdot V}{\overline{p}_{\mathrm{OffDesign}} \cdot V} = \frac{m \cdot R \cdot \overline{T}_{\mathrm{CR}}}{m \cdot R \cdot \overline{T}_{\mathrm{OffDesign}}}. \tag{2}$$

With the assumption of a constant volume of all pipes, heat exchangers, etc. and a constant mass of nitrogen, this equation can be simplified and determining the average pressure in the secondary cycle to

$$\overline{p}_{\mathrm{OffDesign}} = \overline{p}_{\mathrm{CR}} \cdot \frac{\overline{T}_{\mathrm{OffDesign}}}{\overline{T}_{\mathrm{CR}}}. \tag{3}$$

3.2 Liquid Hydrogen Pump

For the calculation of conventional components in gas turbine systems e.g. compressors, turbines, and nozzles, well established methods already exist [20] and are also used in this work. However, cryogenic pumps designed for liquid hydrogen represent a completely new component in aviation. Therefore, the modeling approach applied for these pumps is described in detail below. A generic operating map is used for the pump because its concrete geometry is not available at this point. The generic map is scaled analogous to the scaling approach for compressors. A distinction is made between a design calculation and an off-design calculation. At the design point a pressure ratio and an efficiency are prescribed. These values are selected so that the requirements of the fuel system are satisfied with particular emphasis on the pressure ratio, see Section 3.1. The component map is scaled to match the design point requirements and is used during off-design calculations. The scaling procedure requires, in addition to the pressure ratio, a relative rotational speed and a coordinate to position the design point in the map, as demonstrated for compressors by Kurzke [20]. The resulting scaled map for the liquid hydrogen pump is illustrated in Fig. 2. This performance map has the pressure ratio on the ordinate and the relative mass flow on the abscissa. Lines of constant relative rotational speed define the operating range of the pump.

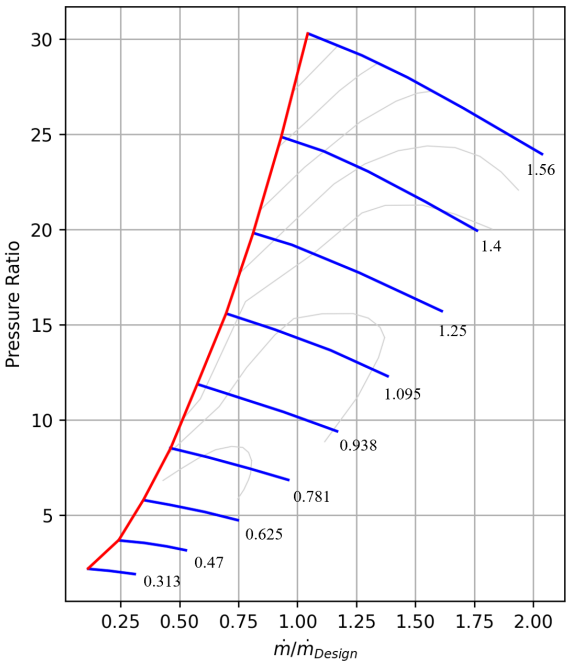


Figure 2 – Liquid hydrogen pump map [21]

Due to the novelty of these pumps in aviation, there are hardly any performance maps in the literature available. The performance map shown originates from the MARK 48-F centrifugal turbo pump used in space rockets [21]. The use of a cryogenic pump in space travel is subject to completely different requirements. For example, significantly higher mass flows (2.74 kg/s) are delivered and shorter operating times (10 hours accumulated run time) are required design conditions [22].

3.3 Heat Exchanger

All modeling methods for the heat exchangers focus on the transferred heat to extract the impact of the respective method. Pressure losses are more dependent on integration aspects which are not taken into account at this point. All pressure losses are set to an individual value for the design point and correlations, as a function of the reduced mass flow, are used to evaluate the pressure loss in different operating conditions.

3.3.1 Correlations

A distinction is made between the design and off-design calculation. Simplified equations for heat transfer are used. It is important to note that this method does not involve any preliminary design of the heat exchanger. The aim is to model the operating behavior with the correct trends for different inlet conditions at all operating conditions of the engine. The transferred heat is specified at the design point. Either as the actual amount of heat in watts or as a dimensionless variant, e.g., as an effectiveness. The effectiveness is defined in equation 4

$$\varepsilon = \frac{\dot{Q}}{\dot{Q}_{\max}}. \tag{4}$$

Here, $\dot{Q}_{\max}$ corresponds to the maximum possible amount of heat at which the outlet temperature of one side equals the inlet temperature of the other side. This value can be calculated for both sides but the smaller value is valid for this equation. Once the amount of transferred heat is known, the entire temperature profile of the heat exchanger is known. Using the logarithmic mean temperature for a counterflow heat exchanger, the heat transfer capability kA can be determined from equation 5

$$\dot{Q} = kA \cdot \Delta T_{\ln}. \tag{5}$$

Here, k corresponds to the overall heat transfer coefficient and A to the transfer area. Overall, kA can be understood as the size of the heat exchanger. By simplifying that both sides of the heat exchanger have the same area and neglecting the thermal resistance of the walls, equation 6 can be applied. The α_i corresponds to the heat transfer coefficient of one side.

$$\frac{1}{k} = \frac{1}{\alpha_{\text{inner}}} + \frac{1}{\alpha_{\text{outer}}}. \tag{6}$$

Using the Nusselt number Nu_i, it is possible to determine the respective α_i, see equation 7. Here, λ is the thermal conductivity and L the characteristic length

$$\alpha_i = \frac{Nu_i \cdot \lambda}{L}. \tag{7}$$

Correlations from [23] are used to calculate the Nusselt number. Only tube bundle heat exchangers are modeled in this paper. The corresponding correlations are given below.

Outer Side: Tube bundle

$$Nu = 0.3 + \sqrt{Nu_{\text{lam}}^2 + Nu_{\text{turb}}^2} \tag{8}$$

$$Nu_{\text{lam}} = 0.664 \cdot \sqrt{Re} \cdot \sqrt[3]{Pr} \tag{9}$$

$$Nu_{\text{turb}} = \frac{0.037 \cdot Re^{0.8} \cdot Pr}{1 + 2.443 \cdot Re^{-0.1} \cdot (Pr^{2/3} - 1)} \tag{10}$$

Inner Side: Tube flow

For $0.5 \leq Pr \leq 1.5$

$$Nu = 0.0214 \cdot (Re^{0.8} - 100) \cdot Pr^{0.4} \cdot [1 + (d/l)^{2/3}] \tag{11}$$

and for $1.5 < Pr < 500$

$$Nu = 0.012 \cdot (Re^{0.87} - 280) \cdot Pr^{0.4} \cdot [1 + (d/l)^{2/3}] \tag{12}$$

Using the given equations, it is now possible to calculate the heat exchangers both in design and off-design. During the design calculation, the amount of heat is specified. Subsequently, the transfer area A can be determined using equations 5 - 12. For this purpose, assumptions regarding the geometry must be made. The pipe diameters or pipe lengths are needed, as these are required to calculate the Reynolds number. The area A is constant for the entire operating range, whereby the heat transfer coefficients will change. During an off-design operating point, the amount of heat transferred can be solved iteratively.

3.3.2 Heat Exchanger Map

Scalable heat exchanger maps were presented by Görtz et. al. [24] for the use in engine performance studies. They have the advantage of not needing a geometry. The presented engine concept was an inter-cooled turbofan engine and the heat exchanger map was developed for exactly this application. Hydrogen was used as a heat sink for the air between booster and high-pressure compressor. This type of map was adapted to the Exhaust HEX for the presented engine concept. Similar to a compressor map, where the pressure ratio is mapped for a set of rotational speeds and mass flows, the heat flux in the heat exchangers is mapped as a non-dimensional effectiveness for a set of mass flows and inlet temperature difference. Therefore, the effectiveness in Equation 13 is used as a value for the ordinate in the heat exchanger map

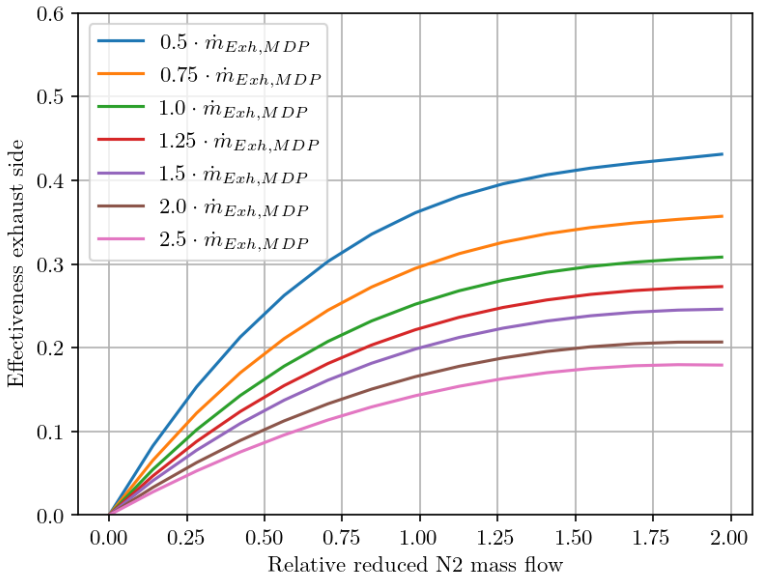


Figure 3 – Heat exchanger map for the Exhaust HEX

$$\varepsilon = \frac{\dot{Q}}{\dot{Q}_{\text{Max,Exhaust}}}. \tag{13}$$

In this equation, $\dot{Q}$ is the heat flux and $\dot{Q}_{\text{Max,Exhaust}}$ is the maximum amount of heat flux of the exhaust side. $\dot{Q}_{\text{Max,Exhaust}}$ is reached when the outlet temperature of exhaust side equals the inlet temperature of the nitrogen side. Thus, an effectiveness of 1 means that the heat exchanger is transferring the maximum possible heat. To allow a 2D representation of the map, the main influencing values are used. The exhaust mass flow is plotted as a family of curves analogous to compressor rotational speed lines. The abscissa of the map is represented using a reduced mass flow rate $\dot{m}_{\text{Red, N2}}$, see Equation 14. This is the product of the nitrogen mass flow and the inlet temperature difference

$$\dot{m}_{\text{Red, N2}} = \dot{m}_{\text{N2}} \cdot (T_{\text{Exhaust,In}} - T_{\text{N2,In}})^n. \tag{14}$$

This reduction is chosen because the mass flow rate and the temperature difference have the highest impact on the heat transfer. In addition, a calibration exponent n is required to allow for map adjustment. An exponent of $n = 0.25$ was proposed by Görtz et. al. and this value is used for the presented studies [24]. The map is also normalized and the design point corresponds to 100 % exhaust mass flow and 100 % reduced nitrogen mass flow. The effectiveness ε itself is already dimensionless. The normalized heat exchanger map is shown in Figure 3. At this position an effectiveness of 0.25 in plotted. This value is a direct result from Equation 1 because the transferred heat can be used to calculate the effectiveness.

The heat exchanger map in the literature is scalable and could be used directly for the Exhaust HEX. However, the application and boundary conditions are different, which would result in significant scaling errors. To minimise scaling errors, a new map was created for use with the presented engine concept. This map was created using the PreHEAT tool (see Section 3.3.3) and no scaling is required. The inlet conditions for the heat exchanger are provided by reference engine performance calculations. This data set includes the secondary nitrogen cycle and consists of multiple operating points and working lines at sea level and under flight conditions. This includes minimum and maximum values for the exhaust and nitrogen mass flow rates and temperatures. The $\dot{m}_{\text{Red, N2}}$ combines the nitrogen mass flow rate and both inlet temperatures. The minimum value of the $\dot{m}_{\text{Red, N2, min}}$ for the map is a combination of all the minimum values, and the same approach is used for the maximum values. The heat exchanger map is created between the boundaries of the $\dot{m}_{\text{Red, N2}}$ and $\dot{m}_{\text{Exhaust}}$. The effectiveness is then calculated using PreHEAT to create the map.

3.3.3 PreHEAT

PreHEAT is a tool developed for the preliminary design and analysis of heat exchangers in aerospace applications at the German Aerospace Center. The methodology implemented in this tool has already been validated against selected reference test cases [25]. In addition to the simulation of stand-alone heat exchangers, the tool has also been successfully integrated into aero engine performance simulations [26]. The underlying modeling approach is based on a cell-based NTU (Number of Transfer Units) method, in which individual cells can be interconnected in an arbitrary manner. Within each cell, the governing equations of the NTU method are solved locally. This enables an accurate prediction of heat exchanger performance while simultaneously providing spatially resolved results across the heat exchanger domain. A schematic representation of the implemented approach is shown in Figure 4.

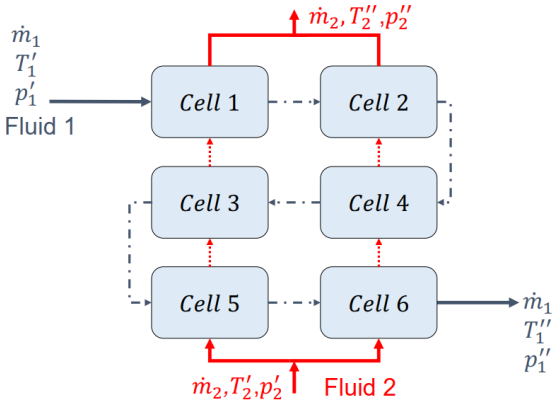


Figure 4 – PreHEAT cell based approach [25]

For the heat exchanger calculations, PreHEAT requires a predefined geometric configuration. In the case of the Exhaust HEX, this includes parameters such as tube diameter, number of tubes, tube length, tube arrangement, and tube spacing. Within the present work, a cross-counterflow heat exchanger configuration implemented as a shell-and-tube heat exchanger is considered. Nitrogen flow through the inner side of the tubes and the exhaust flows though the outer side of the tube bundle. The number of tubes as well as the tube length are adjusted iteratively until the required heat transfer rate obtained from the reference calculation is achieved.

4. Results

The three presented heat exchanger methods, correlations, map and PreHEAT, are applied to calculated the same exhaust heat exchanger for the same operating conditions. The obtained results are compared and evaluated against each other on both, component level and engine level. For all simulations performed using PreHEAT, a single heat exchanger geometry was used throughout the analysis. This geometry corresponds to the configuration that provides the required heat transfer rate under cruise flight conditions. Likewise, the same heat exchanger map was used for all calculations based on the map approach. No additional scaling of the map was required, since it had been generated using the identical geometry employed in the PreHEAT simulations.

4.1 Component level comparison

This section presents the comparison of the heat exchanger methods on component level. The objective is to systematically evaluate the influence of the most relevant inlet parameters on the calculated heat exchanger performance. For this purpose, the mass flow rates and inlet temperatures are varied individually and each modeling method is applied accordingly. The results of this comparison are shown in Figures 5 and 6, where the transferred heat is plotted as a function of the respectively varied parameter. Cruise conditions are used as the reference operating point. Both the heat exchanger map and the PreHEAT geometry were designed based on this operating condition. Furthermore, the

correlations were applied in such a way that the required heat transfer rate is achieved at the reference point. Consequently, all curves intersect at the reference operating condition.

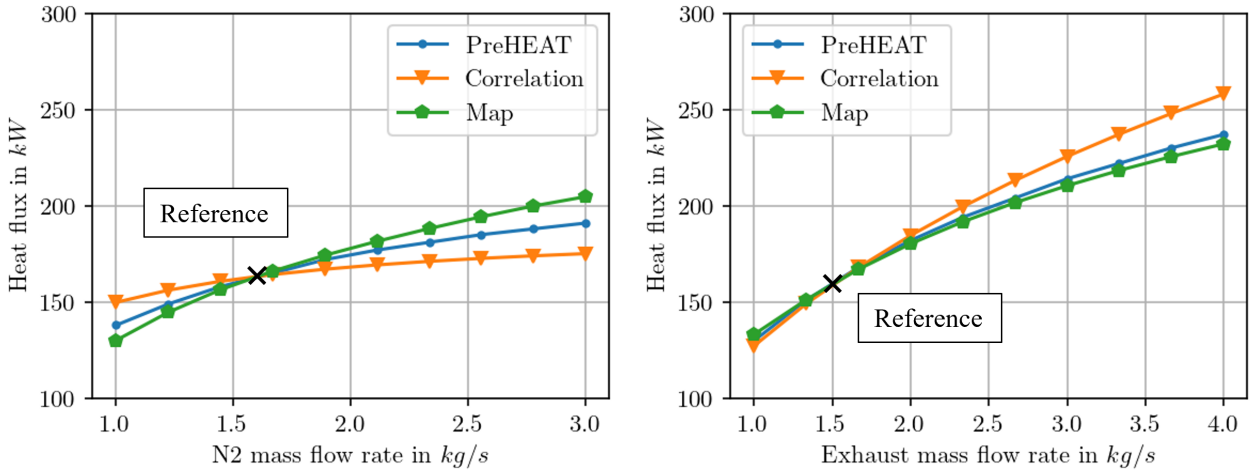


Figure 5 – Comparison of HEX methods for different mass flow rates

Figure 5 shows the influence of the mass flow rates on the heat flux. Since the exhaust heat exchanger is the focus of this comparison, both the nitrogen mass flow rate and the exhaust gas mass flow rate are varied. All modeling methods capture the same general trend. An increase in mass flow rate results in an increased heat transfer. This behaviour is expected, as the heat transfer coefficient is proportional to the Reynolds number. The Reynolds number increases with higher flow velocity and consequently with higher mass flow rate. This relationship applies to both fluid sides of the heat exchanger. For variations in the nitrogen mass flow rate, the correlations show the lowest sensitivity, whereas the heat exchanger map exhibits the strongest response. The PreHEAT method lies between these two methods. As a result, the map-based method predicts the highest heat transfer rates at higher nitrogen mass flow rates and the lowest heat transfer rates at lower nitrogen mass flow rates. The abscissa of the map is defined as a combination of the N2 mass flow rate and the inlet temperature difference. During the generation of the map, both parameters were varied simultaneously. In the present study only the N2 mass flow rate is varied. As a consequence, the map implicitly assumes a corresponding variation in the inlet temperature difference, leading to an overestimation of the heat exchanger effectiveness and heat transfer rates compared to the values predicted by PreHEAT. Furthermore, PreHEAT employs its own set of embedded correlations, which require a larger number of input parameters. These correlations differ from those applied in the present work, resulting in the observed discrepancies between the two methods. In contrast, the opposite behaviour can be observed for variations in the exhaust gas mass flow rate. In this case, the correlations react most strongly to changes in exhaust gas mass flow. Consequently, the correlations predict the highest heat transfer rates for increased exhaust gas mass flows and the lowest heat transfer rates for lower exhaust gas mass flows. The variation of the exhaust gas mass flow rate is explicitly represented within the map. Consequently, the results obtained from PreHEAT and the map show very good agreement, with the corresponding curves lying close to one another. However, the correlation method in the present study were developed for general tube bundle heat exchangers. Since the geometry considered here consists of only a small number of tubes, deviations arise between the correlations predictions and the results obtained with PreHEAT.

Figure 6 shows the influence of the inlet temperatures on the heat transfer. A linear trend can be seen, which is represented similarly by all three modeling methods. At very low nitrogen inlet temperatures noticeable deviations occur. These deviations are caused by the strongly varying thermophysical properties of nitrogen in this operating region. Due to its high pressure, the nitrogen is in a supercritical state. However, the low inlet temperatures are close to the critical point and the two-phase region, where significant variations in properties such as density, thermal conductivity and specific heat capacity occur. This effect is captured by PreHEAT and the correlations, since the fluid properties are

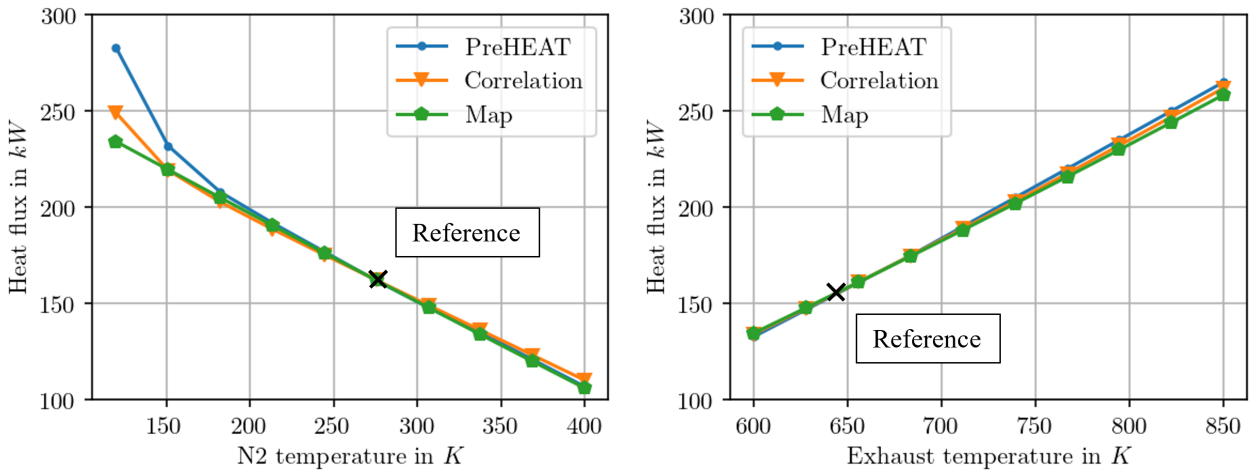


Figure 6 – Comparison of HEX methods for different inlet temperatures

calculated using CoolProp [27]. In contrast, the heat exchanger map does not reproduce these gradients, as the map was generated only for operating conditions with higher nitrogen temperatures. However, except for this region all methods provide comparable results. Increasing the nitrogen inlet temperature reduces the temperature difference between both fluid sides of the heat exchanger. As the heat sink temperature increases, the driving force for heat transfer decreases, resulting in a lower transferred heat. An analogous behaviour is shown for the exhaust gas temperature. Higher exhaust gas inlet temperatures increase the temperature difference between both fluid sides of the heat exchanger, leading to an increased heat transfer.

In summary, all methods reproduce the overall trends consistently on component level. Regarding the influence of the mass flow rates, the heat exchanger map method shows the highest sensitivity to variations in the nitrogen mass flow rate, whereas the correlations react most strongly to changes in the exhaust gas mass flow rate. In both cases, PreHEAT provides intermediate results between the two methods. The trends associated with variations in the inlet temperatures are captured well by all methods. However, the influence of the selected modeling method on the predicted heat transfer rate is less pronounced.

4.2 System level comparison

The following section presents a comparison of the heat exchanger methods at engine level. The thermodynamic cycle of the same engine, designed according to identical design rules, is calculated using each heat exchanger modeling method. The different methods are applied to the Exhaust HEX, all remaining heat exchangers are modeled exclusively using the correlation based method. It should be noted that all results are identical under cruise conditions. During cruise, the heat transfer rate is prescribed. In the case of simulations using PreHEAT as the heat exchanger modeling method, a geometry is required that has been designed to achieve this specified heat transfer rate. Table 2 presents the results for the operating points MTO and TOC. Selected values for the correlation based method are shown together with the deviations obtained from the map method and the PreHEAT calculation.

The differences between the investigated methods are very small for the selected system variables. The predicted temperatures and fuel consumption differ by no more than 0.03 %, indicating a very high level of agreement between the approaches. Slightly larger deviations are observed for the parameters of the secondary cycle. In particular, the differences between the correlation-based approach and the performance map method reach up to 1.6 % at MTO and 4.0 % at TOC for the effectiveness of the exhaust gas heat exchanger. By comparison, the deviations between the correlation-based model and the PreHEAT calculation amount to 1.1 % at MTO and 0.66 % at TOC. These differences in the heat exchanger modeling also affect other performance indicators of the secondary cycle, such as the mass flow rate in the nitrogen loop and the associated compressor power con-

Table 2 – Comparison of Correlation vs Map Method

		MTO			TOC		
	Unit	Correlation	Δ Map %	Δ PreHEAT %	Correlation	Δ Map %	Δ PreHEAT %
TSFC	$g/kN/s$	2.51	0.011	0.007	5.17	0.03	0.005
T_{41}	K	1820.9	-0.002	-0.002	1700.5	-0.01	-0.002
T_5	K	817.0	-0.001	-0.002	697.9	-0.005	-0.002
T_{201}	K	342.8	-0.37	-0.12	290.7	-0.77	-0.12
$\dot{Q}$	kW	374.7	-1.3	-1.0	200.6	-3.5	-0.58
ε	-	0.175	-1.6	-1.1	0.26	-4.0	-0.66
$\dot{m}_{N2}$	kg/s	2.62	-0.35	-0.14	2.09	-0.6	-0.1
$P_{Compressor}$	kW	120.6	-0.33	-0.45	93.1	-0.85	-0.29

sumption. This behavior can be explained by the change in temperature T 201, which results from the modified heat transfer rate and consequently influences the pressure within the nitrogen cycle, as described by Equation 3. Overall, the deviations between the correlation-based approach and the PreHEAT results are smaller than those between the correlation-based approach and the performance map method. The larger discrepancies associated with the performance map method are particularly noticeable under TOC operating conditions.

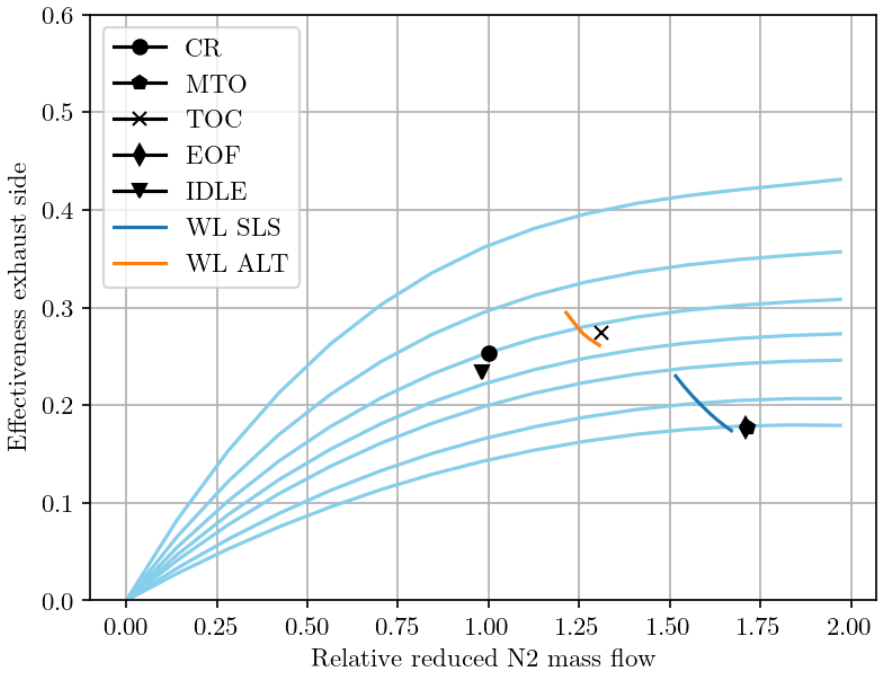


Figure 7 – Heat exchanger map with operating points for the map method

Figure 7 illustrates the operating points included in the map. In addition, the idle condition, end-of-field condition, and two working lines (WL) at sea level static (SLS) and altitude (ALT) are shown. The WL ALT corresponds to thrust settings between 18 kN and 28 kN, whereas the WL SLS covers thrust settings between 70 kN and 140 kN. For both WLs, a temperature above ISA of 0 was assumed, resulting in a slight discrepancy between TOC and the WL ALT, as well as between MTO and WL SLS. The nitrogen mass flow rate is primarily controlled by the compressor rotational speed. Since the corrected compressor speed was maintained constant throughout the entire operating range, the nitrogen mass flow rate varies only slightly. Consequently, the value on the abscissa also exhibits only minor variation across the considered operating conditions.

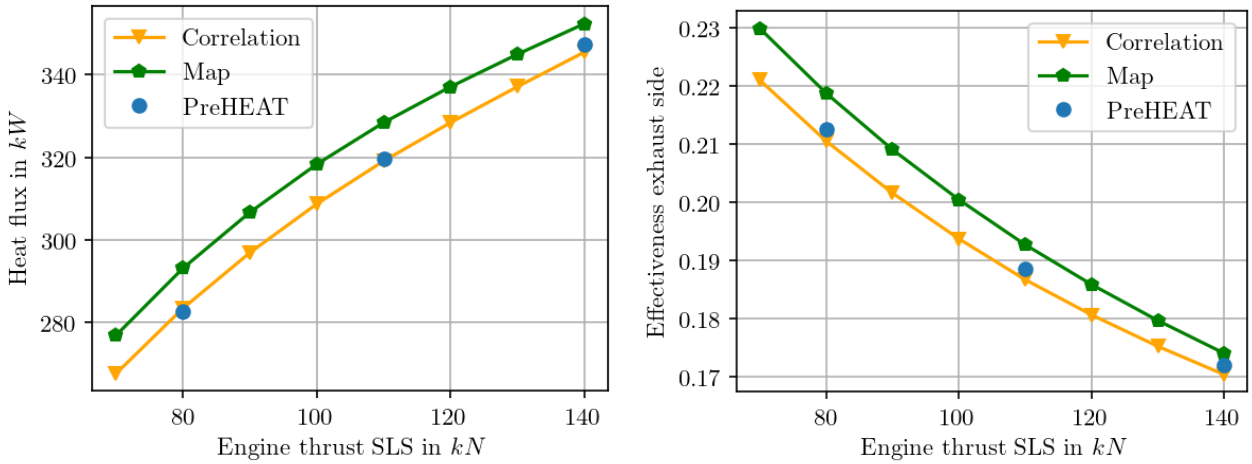


Figure 8 – Heat exchanger behavior in system for working line

Figure 8 presents the heat transfer and effectiveness of the exhaust HEX for the SLS working line. The results from the correlations, the map, and PreHEAT are shown together. PreHEAT and the correlations results are in very close agreement, which might not be expected based on component-level comparisons. However, the effects tend to cancel each other out: while the correlations underestimate the heat transfer for higher nitrogen mass flows, they overestimate it for higher exhaust mass flows. Along the operating line, both mass flows are increased compared to the reference, resulting in a very close match between these two methods. On the other hand, the map consistently overestimates both the heat transfer and the effectiveness of the exhaust HEX across the entire working line, introducing a noticeable offset.

Overall, the calculations using the correlations show good agreement with the PreHEAT results. However, the map deviates more at certain points. This is primarily due to the way the map was constructed. Each point in the map was initially calculated using PreHEAT. To reduce the dataset to a 2D format, suitable for visualization, a reduced mass flow was introduced, which depends on the nitrogen mass flow and the inlet temperatures on both sides. Consequently, the same reduced mass flow can be achieved under different fluid conditions. During the creation of the performance map, the combination of inlet temperatures and mass flows differed from those encountered, for example, at TOC and along the working line. Although this leads to deviations in heat transfer of 3–4 %, the impact on the overall engine performance calculation is only minor.

5. Conclusions

This work presented an engine and LH2 pre-conditioning concept based on a secondary nitrogen cycle, which reduces the risk of icing. Several approaches are available for modeling heat exchangers. In this study, three methods were presented and investigated: a correlation-based approach, a map approach and the use of the higher-order cell-based simulation tool PreHEAT. The impact of each modeling method on the overall engine cycle was demonstrated using the exhaust gas heat exchanger as a representative example. PreHEAT is considered the reference solution, as it provides the highest level of accuracy and has been validated against experimental data. Based on the conducted analyses, the research questions introduced at the beginning of this paper can be answered as follows:

RQ1: Impact on engine level

The influence of the selected heat exchanger modeling approach on the overall system is negligible. Temperatures, pressures, and fuel consumption differ by no more than 0.03 % between the investigated methods and therefore remain within the uncertainty margins of the analysis. The performance of the overall system is primarily governed by the chosen architecture and operating strategy rather

than by the heat exchanger modeling approach. In contrast, the impact on component-level analyses is more pronounced. Deviations of up to 4 % in the predicted effectiveness of the exhaust gas heat exchanger were observed when using the map approach. Furthermore, an offset in the calculated working lines can be identified, indicating systematic differences between the modeling methods at the component level.

RQ2: Advantages and disadvantages
The advantages and disadvantages of the individual modeling approaches are qualitatively summarized in Table 3. The methods are evaluated based on three criteria: (i) whether geometric information is required, (ii) the achievable accuracy of the results and (iii) the scalability of the approach.

Table 3 – Qualitative method evaluation

	Correlations	**Map**	**PreHEAT**
Geometry independency	+	+	- -
Results	+	-	++
Scalability	++	++	-

Correlations: The correlation-based approach performs well with respect to all three evaluation criteria. Only simplified geometric boundary conditions are required, some of which have little influence on the results, as the overall size of the heat exchanger is adjusted during the design calculation to satisfy the required heat transfer rate. The predicted results show good agreement with those obtained from the PreHEAT simulations. Furthermore, this approach is highly scalable and can therefore be readily applied to different heat exchanger configurations and operating conditions.
Map: The primary advantage of the map approach is that it does not require detailed geometric information while remaining scalable. This makes it particularly well suited for application within engine performance simulations. The results obtained at the engine system level show good agreement with the reference solutions. However, smaller deviations become apparent in component-level analyses. An additional benefit of the map approach is that the representation of operating behavior is easy to understand and can be presented visual in the 2D plot. Nevertheless, the accuracy and applicability of the method strongly depend on how the map is generated. For the application presented by Görtz et. al. [24], the reduction of the map to a single independent variable proved to be effective. However, such a simplification is not possible for the exhaust gas heat exchanger, where the operating behavior is governed by a more complicated set of influencing parameters.
PreHEAT: The use of PreHEAT requires a detailed specification of the heat exchanger geometry. Within the context of engine performance simulations, this represents a drawback, as parameters such as tube diameter, length, and flow configuration must already be defined at an early design stage. As a consequence, the flexibility typically associated with performance-level analyses cannot be fully exploited. However, this approach yields the most accurate results among the investigated methods. Once a specific geometry has been defined, the possibilities for scaling the model are limited, which restricts its applicability to parametric studies or early design space explorations.

RQ3: Recommended method
Overall, both the correlation-based approach and the use of PreHEAT are suitable for thermodynamic cycle analysis. In the early design phase, when large parameter spaces are explored, the flexibility of the correlations is advantageous. This enables the capture of overall trends and supports the resolution of key questions regarding the selection of the LH2 pre-conditioning system architecture. In contrast, once the design transitions into preliminary component design, the use of PreHEAT becomes most appropriate. At this stage, large parameter studies are no longer the primary focus, and the objective shifts towards defining and analyzing a preliminary geometry.

6. Copyright Statement

The authors confirm that they, and/or their company or organization, hold copyright on all of the original material included in this paper. The authors also confirm that they have obtained permission, from the copyright holder of any third party material included in this paper, to publish it as part of their paper. The authors confirm that they give permission, or have obtained permission from the copyright holder of this paper, for the publication and distribution of this paper as part of the ICAS proceedings or as individual off-prints from the proceedings.

References

[1] European Commission. Fly the green deal: Europe's vision for sustainable aviation.

[2] Daniel G. Brewer. *Hydrogen aircraft technology*. CRC, Boca Raton, 1991.

[3] Andreas Westenberger. Liquid hydrogen fuelled aircraft - system analysis. *CRYOPLANE, The European Commission, Brussels, Belgium, Report No. GRD1-1999-10014*, 2003.

[4] Alexandre Capitao Patrao, Isak Jonsson, Carlos Xisto, Anders Lundbladh, and Tomas Grönstedt. Compact heat exchangers for hydrogen-fueled aero engine intercooling and recuperation. *Applied Thermal Engineering*, 243:122538, 2024.

[5] Hiroki Masuda, Ryosuke Oshima, Daisuke Kato, Tomoko Tsuru, Yoshiaki Kusumoto, Yasuhiro Kinoshita, Ryoichi Onishi, Koji Iwahara, and Hiromasa Hayashi. Progress on hydrogen combustion engine technologies in innovative japanese hydrogen aircraft project. *Proceedings of ASME Turbo Expo 2026*, 2026.

[6] Alexander Görtz and Daniel Silberhorn. Thermodynamic potential of turbofan engines with direct combustion of hydrogen. *International Council of the Aeronautical Sciences (ICAS)*, (33rd Congress), 2022.

[7] Stefano Boggia and Klaus Rüd. Intercooled recuperated gas turbine engine concept. In *41st AIAA/ASME/SAE/ASEE Joint Propulsion Conference & Exhibit*, Reston, Virigina, 2005. American Institute of Aeronautics and Astronautics.

[8] Henrik Gonser. Untersuchung zum einsatz von wärmetauschern in zivilen turboflugtriebwerken. *Universität Stuttgart*, 2008.

[9] Oliver Schmitz, Hermann Klingels, and Petra Kufner. Aero engine concepts beyond 2030: Part 1—the steam injecting and recovering aero engine. *Journal of Engineering for Gas Turbines and Power*, 143(2), 2021.

[10] Paul Ziegler, Sascha Kaiser, and Volker Gümmer. Parametric cycle studies of the water-enhanced turbofan concept: Gt2023-100529. In *Proceedings of ASME Turbo Expo 2023: Turbomachinery Technical Conference and Exposition (GT 2023)*, New York, N.Y., 2023. the American Society of Mechanical Engineers.

[11] Philip P. Walsh and Paul Fletcher. *Gas turbine performance*. Blackwell Science, Oxford, 1998.

[12] Christian Klumpp, Daniel Weintraub, and Peter Jeschke. Cryogentic hydrogen aero engine performance calculations. *Proceedings of ASME Turbo Expo 2026*, 2026.

[13] Mehdi Anhichem, Konstantinos Bollas, Georgios Arvithis, Vasilis Gkoutzamanis, Vito Tagarielli, and Anestis Kalfas. Advancing safety and robustness of thermal management architectures for future hydrogen propulsion. *Proceedings of ASME Turbo Expo 2026*, 2026.

[14] Petter Miltén, Isak Jonsson, Anders Lundbladh, Marcus Wiegand, and Carlos Xisto. Performance estimation of application-suited heat exchangers. *Proceedings of ASME Turbo Expo 2026*, 2026.

[15] Christina Salpingidou, Dimitrios Misirlis, Zinon Vlahostergios, Michael Flouros, Stefan Donnerhack, and Kyros Yakinthos. Numerical assessment of the performance of a heat exchanger for a low pressure ratio gas turbine. *Energy*, 164:171–182, 2018.

[16] Richard Becker, Florian Wolters, Mobin Nauroz, and Tom Otten. Development of a gas turbine performance code and its application to preliminary engine design. *Deutscher Luft- und Raumfahrtkongress DLRK*, 2011.

[17] Stanislaus Reitenbach, Alexander Krumme, Thomas Behrendt, Markus Schnös, Thomas Schmidt, Sandrine Hönig, Robert Mischke, and Erwin Mörland. Design and application of a multidisciplinary predesign process for novel engine concepts. *Journal of Engineering for Gas Turbines and Power*, 141(1), 2019.

[18] S. Reitenbach, M. Vieweg, R. Becker, C. Hollmann, F. Wolters, J. Schmeink, T. Otten, and M. Siggel. Collaborative aircraft engine preliminary design using a virtual engine platform, part a: Architecture and methodology: Aiaa 2020-0867. *AIAA Scitech Forum*, 2020.

[19] Alexander Görtz, Jannik Häßy, Marc Schmelcher, Mahmoud El-Soueidan, and Florian Herbst. Integration of a conditioning system for liquid hydrogen into the performance model of a turbofan engine using a secondary fluid. *Proceedings of ASME Turbo Expo 2026*, 2026.

[20] Joachim Kurzke. *Propulsion and Power: An Exploration of Gas Turbine Performance Modeling*. Springer International Publishing AG, Cham, 2018.

[21] Joseph P. Veres. Centrifugal and axial pump design and off-design performance prediction. *National Aeronautics and Space Administration*, 1994.

[22] A. Csomor and R Sutton. Small, high-pressure liquid hydrogen turbopump. *National Aeronautics and Space Administration*, 1977.

[23] *VDI-Wärmeatlas*. SpringerLink Bücher. Springer Vieweg, Berlin, Heidelberg, 11., bearb. und erw. aufl. edition, 2013.

[24] Alexander Görtz, Konstantinos Kyprianidis, and Dimitrios Bermperis. Implementation of intercompressor cooling in the cycle analysis of hydrogen powered gas turbine engines using scalable heat exchanger maps. *Journal of Engineering for Gas Turbines and Power*, 147(12), 2025.

[25] Marc Schmelcher, Jannik Häßy, Alexander Görtz, and Mahmoud El-Soueidan. Methods for the preliminary design of heat exchangers in aircraft engines. In *Proceedings of ASME Turbo Expo 2023: Turbomachinery Technical Conference and Exposition (GT 2023)*, New York, N.Y., 2023. the American Society of Mechanical Engineers.

[26] Marc Schmelcher, Jannik Häßy, Alexander Görtz, Mahmoud El-Soueidan and Fabian Nöske. Integration of heat exchanger models into the performance analysis of innovative aero engine architectures. *Proceedings of International Society for Air Breathing Engines (ISABE)*, 2024.

[27] Ian H. Bell, Jorrit Wronski, Sylvain Quoilin, and Vincent Lemort. Pure and pseudo-pure fluid thermophysical property evaluation and the open-source thermophysical property library coolprop. *Industrial & Engineering Chemistry Research*, 53(6):2498–2508, 2014.